2021 IEEE/RSJ International Conference on Intelligent Robots and Systems (IROS)
September 27 - October 1, 2021. Prague, Czech Republic

2021 IEEE/RSJ International Conference on Intelligent Robots and Systems (IROS) | 978-1-6654-1714-3/21/$31.00 ©2021 IEEE | DOI: 10.1109/IROS51168.2021.9636771

A Soft Assistive Device for Elbow Effort-Compensation

Emir Mobedi[1,2], Wansoo Kim[1], Elena De Momi[2], Nikos G. Tsagarakis[1], and Arash Ajoudani[1]

***Abstract*— The use of assistive technologies in industrial environments to improve human ergonomics and comfort in repetitive and high effort tasks have increased considerably in the last decade. Predominantly, the goal is to provide additional physical support through lightweight and wearable devices, without posing major constraints to the human body movements. Towards achieving this objective, in this work we present a novel actuation mechanism for a soft assistive device, by taking into account the human elbow torque-angle profile. The proposed design integrates a single motor coupled with an elastic bungee and a cam-spool mechanism to enable energy exchange during the elbow flexion movement, while allowing for free-motions during the extension of the joint. A cable-driven transmission with passive elastic attachments is employed to implement compliant couplings with the wearer and to achieve easy donning/doffing. Experiments are conducted on two 3D printed functional prototypes. Results suggest that the assistive elbow torque is effectively transmitted with an average 90% success for balancing a 5N payload, and the free-motion range of 108° is measured for both flexion and extension.**

I. Introduction

Robotic exoskeletons are wearable mechanical devices designed to enhance the physical performance of the wearer, or to assist him/her to regain a weakened or lost functionality [1]. Example applications range from load carrying [2] and tool use [3], to motion assistance in sit-to-stand [4] and walking [5] tasks. In particular, the use of robotic exoskeletons in industrial applications has shown great promise for preventing work-related musculoskeletal disorders, representing the largest category of occupational diseases worldwide.

To create active devices that are functional, yet also safe and ergonomic for the target applications, several requirements related to the wearer's comfort and safety, low mass/inertia, range of motion, easy wearability, and force range [6] must be met in the design stage. For instance, for what concerns the users' comfort when using such systems in industrial applications, rigid exoskeletons seem to have little potential due to the common misalignment of the exoskeleton joints with those of the human [7]. Such a misalignment eventually can result in the generation of parasitic forces and constraints in the motion of the human joints, and generate discomfort. Solving the problem of misalignment in a rigid exoskeleton requires the incorporation of additional degrees of freedom in the kinematic chain of the device [8], [9], or the inclusion of adaptive actuation systems (e.g., series elastic actuation (SEA) [10], [11]), resulting in a higher, unwanted complexity. Although this increased complexity may not be an issue for some rehabilitation systems that operate at a fixed place it prohibits the use of these systems in more mobile applications within the industry, where workers have to wear and walk with these devices within their workplace.

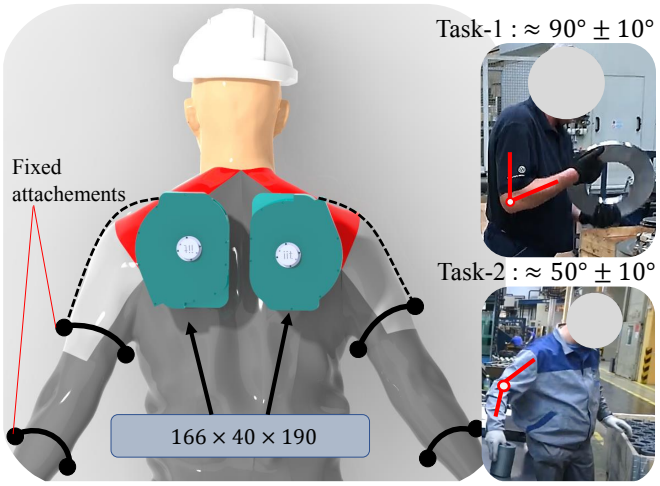

Fig. 1. The concept design of the proposed effort-compensation device, and the kinematic requirements of the targeted heavy material handling task. Dimensions of the device are reported in millimeters. The dashed lines represent the Bowden cables.

To overcome the drawbacks of rigid exoskeletons, several alternative designs have been proposed. Soft exosuits, as a recent design trend, do not constrain the motion of human joints since all interfaces and transmissions of the assistive forces to the human body are implemented through tendon driven mechanisms and elastic elements. The general idea of these devices is to locate the actuation system proximally and to transmit the force via Bowden cables [12]. In this way, the load and the reflected inertia at the supported joints can be reduced during the execution of physical tasks, while increasing the comfort of the wearer. Due to the their low weight, compact structure, and low power consumption ability, they have found several applications targeting the activities of daily living: the authors in [13] proposed an assistive suit through the combination of fabrics attached to the human arm. The device is actuated using an agonist/antagonist motorized actuator with a planetary reduction drive located at the upper back of the human. The work in [14] explored the under-actuation principle to support the elbow joint of both arms using a single DC motor coupled with two pinion-bevel gear systems. The clutch and brake subsystems were used to enable an independent control of the two arms

[1]Istituto Italiano di Tecnologia, Genoa, Italy.
[2]Department of Electronics, Information and Bioengineering, Politecnico di Milano, Milano, Italy.
{emir.mobedi, wan-soo.kim, nikos.tsagarakis, arash.ajoudani}@iit.it

This work was supported by the European Union's Horizon 2020 research and innovation programme under Grant Agreement No. 871237 (SOPHIA).

from the single actuation unit. These additional components and their integration have increased the complexity of the device, despite the fact that only one actuator was used for both elbow joints. Furthermore, since the implementation of this device does not include an elastic element in the actuation/transmission system, it cannot store energy during the flexion or extension movement of the elbow joint. As another option, there are pneumatic actuation-based upper-limb exoskeletons [15], [16] to support the elbow joint. However, the air tank that is needed to actuate the device limits the mobility of the wearer in industrial applications.

Despite the progress made in the area of soft exoskeletons, there is still a need to develop a wearable device for the elbow joint that is cable-driven, lightweight, and easily wearable, which also contains energy storage and adaptive elements to make it suitable for industrial applications. To respond to these design requirements, in this paper, we develop a novel elbow assistive device, whose concept is illustrated in Fig. 1. The device is composed by a novel actuation system that is remotely placed at the upper back of the user's body in order to reduce the weight of the device distributed across the human arm.

To design the actuation system, first, we calculate the desired torque trend of the elbow joint to balance a load at hand. A bungee is selected as the elastic element, to provide an intrinsically soft interaction between the actuation system of the device and the elbow, and to form a mechanical filter against dynamic uncertainties. This choice is due to the intrinsic damping, and the high energy storage density due to a larger elongation possibility (especially w.r.t. metal springs). To adapt the S-shaped force profile of the bungee [17] to the desired torque profile of the human elbow, which is sine shaped, a new optimised cam-spool design is presented. To evaluate the performance of the integrated system, two tests are conducted on a 3D fabricated elbow prototype to evaluate the motion and torque response of the assistive device.

The rest of the paper is structured as follows. In section II and III, the design requirements of the assistive device, the working principle, and the details of the mechanical design are explained. In section IV, the experiments are described and the results obtained from these experiments are presented. Finally, conclusions and future work are discussed in section V.

II. Design Concept & Requirements

The design process of the proposed device involves four main steps dedicated to i) the definition of the required torque and motion range of the elbow, ii) the selection of the elastic element incorporated in the device, iii) the design of the cam-spool mechanism, and finally, iv) the analysis of the working principle of the whole system, which clarifies how the aforementioned steps are integrated into the proposed assistive device system for industrial applications.

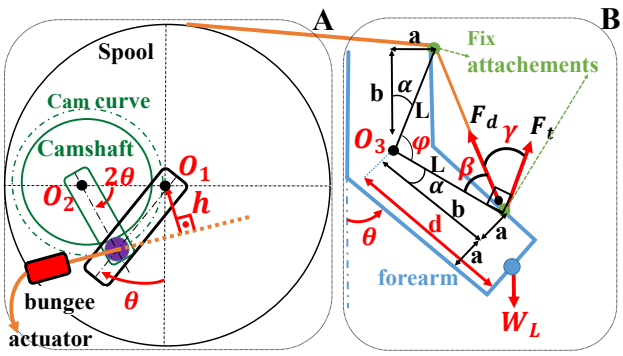

Fig. 2. The illustration of the working principle of the actuation system (A) and the arm attachments (B). The forearm width (a), the distance of fixed attachments from O_3 (b), and the forearm length (d) are determined as 50, 100, and 150 mm, respectively [18].

A. Torque and Motion Range of the Elbow

The goal of this section is to estimate the required elbow torque around O_3 (see Fig. 2B), which is the rotation center of the elbow. Assuming that a payload W_l is applied at the center of mass of forearm, and θ is the elbow angle, the required elbow torque to support to payload is given by:

$$\tau = W_l \sin\theta(d). \tag{1}$$

Subsequently, the desired force on the cable (represented with orange in Fig. 2B) to apply the above torque is calculated as follows:

$$F_d = \frac{\tau}{L\cos(\gamma)}, \tag{2}$$

where

$$\gamma = 90 - \alpha - (\theta/2). \tag{3}$$

The elbow range of motion was selected by characterizing data from two industrial use cases of the European project SOPHIA[1]. Based on the identified range and the imposed implementation constraints, the joint range of $116°(\theta_{max})$ was considered. This range was also in accordance with former studies on occupational ergonomics [19], [20]. For this joint range, the necessary tendon length (l_f) for the flexion and the extension movements was approximately 178 mm using (4):

$$l_f = \sqrt{2(a^2+b^2)(1-\cos\varphi)}. \tag{4}$$

It is important to note here that, a larger elbow range of motion would require larger sizes of the device pulleys in order to deal with the additional tendon length. This will inevitably result in an increased device volume and weight. In fact, the implementation constraints mentioned before referred to the trade-off between the extra range of motion and the additional tendon displacement that must be dealt with.

[1]https://project-sophia.eu

B. Elastic Material Selection

There are two main reasons to incorporate an elastic element in the actuation/transmission of an elbow assistive device. First, it provides an intrinsically softer interaction between the actuation system of the device and the limb of the human body where the actuation output is applied. In this way, the force transmission from the assistive device to the human body can be accomplished in a compliant way. Another advantage is that, such an elastic element eventually forms a mechanical filter against dynamic uncertainties absorbing sudden motions or possible control issues and protecting both the actuation of the device as well the human subject from feeling such dynamic force transients. Furthermore, the incorporation of an elastic element may enable energy storage and recycling, which could lead to the reduction of energy consumption. Such energetic benefits, however, will require specific types of tasks that involve cyclic motions of the human elbow, which may not be so common, in order to explore the energy recycling.

In this work, we consider the incorporation of a rubber-type elastic element in the form of a bungee cord. This selection choice was driven by a number of performance characteristics of this type of elastic element, including its large elongation, intrinsic damping feature, lightweight property, and low sensitivity in mechanical misalignment. This type of elastic element also permits a variety of configurations such as U shape [17].

In our design, to achieve high force output while maintaining the compactness of the design, the bungee is arranged as an endless ring shape. The stiffness profile of such elastic element stiffness flattens out until $2-3\%$ elongation, then increases rapidly until 6%, and the slope of the increment reduces for the rest (see the details in Section IV). In fact, it is known that the main disadvantage of the bungees can be their S-shaped output force profile [21]. To compensate for this, we design a novel cam-spool system, which is lightweight and can adjust the bungee output force mechanically to adapt to the human elbow torque/angle function (1). The details of the cam-spool design are presented in the following Section.

C. Design of the Cam-Spool Mechanism

The design of the cam-spool mechanism considers two objectives. First, the cam-spool system shall permit a tendon length of 178 mm to be wrapped/released during the flexion/extension movement. Then, it should provide a variable lever length that shapes the torque/angle profile generated by the device to that of the human elbow. A design optimization study of the cam-spool system is performed to achieve this second objective.

As it can be seen in Fig. 3, the cam and the elbow are supposed to perform equivalent angles (θ). In our first proof-of-concept design, $R\sin\theta$ curve is drawn for 116° assuming $R = 40$ mm to obtain the cam profile (see Fig. 3). This graph is divided by 4 equal segments of angle θ to explain the geometrical derivation of cam, and the y axis of each θ segment displays the cam radius that is aimed to be matched with the sinusoidal curve. The circles, whose radii vary by

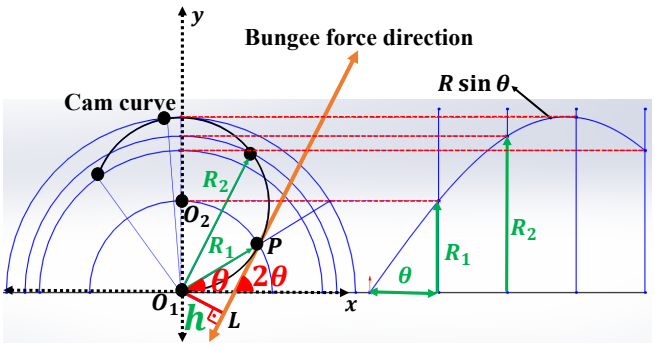

Fig. 3. The illustration of the method to identify cam geometry to match the human elbow torque/angle curve (sine function). The orange line represents the Bowden cable that is connected with bungee elastic material.

$R\sin\theta$ are drawn for each segment of angle θ with respect to the center (O_1). The intersections of circles and divided lines give the point of cam curve, which is a circle (O_2 center) that is shown with black points in Fig 3. Six points and two radii (R_1 and R_2) are illustrated.

To link the obtained cam curve with the human arm and the bungee, two cam-spool implementation cases were evaluated in Fig. 4. In case-1, the rotation axis of the cam (O_2 in Fig. 2 and Fig. 3) and a spool (O_1) are jointed in the same center. On the other hand, in case-2, the rotation axis of the cam and spool are separated. Cam is fixed, and a cable is moved around it via a roller, which is housed in the slot opened in a spool. Considering case-1, when the spool is rotated around O_1, the elongation of bungee will be varied as a function of the cam lever length (h in Fig. 3). However, the direction of the cable, which is connected with bungee, will change for each rotation of the spool since the cam is eccentric (see Fig. 3). This will cause to add extra components into the design to properly constrain the tendon cable. Besides, if the elbow is rotated by θ, the rotation of the spool is supposed to be twice as much to move the cable to the corresponding cam radius. The reason for this motion is that the cable should always be tangent to the cam (see Fig.

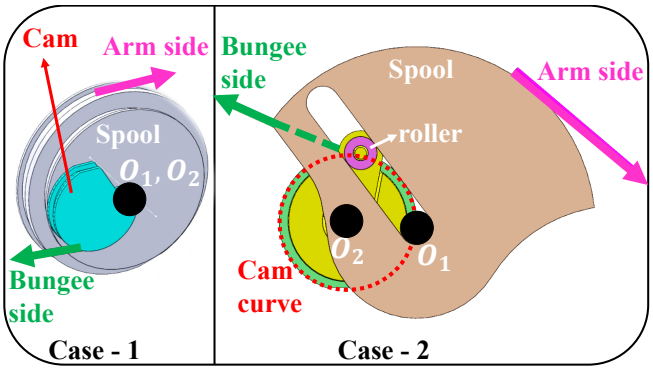

Fig. 4. The cam-spool system alternatives to vary the elastic force with the same trend of human elbow torque/angle profile. Pink and green lines represent the Bowden cables connected to the human arm and the bungee elastic material, respectively. Black points illustrate the center of rotation of the cam and the spool.

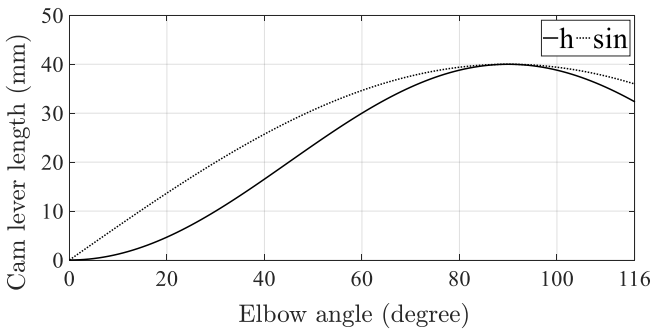

Fig. 5. Geometrically obtained cam lever length (h), and the desired cam profile (sine curve).

3). Hence, the elbow and the spool cannot be synchronized for each rotation of the elbow, and this results in adding a cable transmission into the system that can increase the uncertainties such as friction.

Due to the above mentioned issues of implementation case-1, we adopt an implementation in which the cam is fixed, and the cable is moved around the cam curve through a shaft, whose rotation axis is O_2 (case-2 in Fig. 4). A detailed explanation of how case-2 is integrated into the assistive device is mentioned in the following section.

D. Working Principle

The diagram related to the working principle of the assistive device is presented in Fig. 2A, which includes the camshaft, the spool, and the roller (represented with purple). The camshaft is coupled with the roller, while a slot is opened in the spool. The rotation axis of the camshaft (O_2) and the spool (O_1) are decoupled in order to permit to match the human elbow angle with the corresponding cam lever length. In this way, the spool rotation is in 1:1 relationship with respect to the the elbow angle while the cam link rotates twice as much as the spool. As a result of this coordination, the desired cam lever length (h) can be obtained without adding an extra cable transmission to the system. The torque balance around O_1 can be described by

$$F_{bungee}h = F_{desired}r_{spool}. \tag{5}$$

In (5), cam lever length is calculated from $\triangle O_1LP$ in Fig.3 where R_1 is a function of $R\sin\theta$. Thus:

$$h = R(\sin\theta)^2. \tag{6}$$

As mentioned before, since the tendon cable must be tangent to the cam curve (see Fig. 3), the geometrically acquired cam lever length is not a sinusoidal function.

The proposed assistive device enables the following two functionalities. Under no payload conditions when the elbow joint needs to move without any constraints the roller performs a linear motion in the slot, adapting to the elbow rotation and varying the cam lever length (h) continuously around the spool rotation axis (O_1). In this case, the bungee is tensioned only to avoid relaxation on the cable (to achieve high transparency).

When assistance is needed, the human can take the load with an almost fully extended arm (here, both θ and h have values close to zero). This condition requires a higher elastic force generated by the assistive device to counteract the load according to (5). As the human flexes the elbow, θ and h increase (see Fig. 5), which results in applying less pretension on the elastic element based on (5). In other words, the initially stored elastic force can be adjusted mechanically as a function of the cam lever length during the flexion movement. This is, in fact, one of the significant reasons why the cam-spool system is integrated into the assistive device.

III. Design of Assistive Device Prototype

To validate the functionality of the proposed elbow device, two 3D printed elbow prototypes were produced (see Fig. 8) and tested in two different experiments including fixed-end (elbow-1) and open-end (elbow-2).

The assistive device structure is divided into two sections, the power unit, and the cam-spool system, in Fig. 6. The power unit aims to generate an elastic force to be transferred to the cam-spool system as an input. To achieve this, a Maxon brushless DC motor (EC-4pole 22, 323218) with $5.4:1$ gearbox is coupled with a ball-screw mechanism to move the plate component linearly. An endless ring type of bungee (thickness $\varnothing 5$ mm and initial length 55 mm) mounted on two supports is connected with the camshaft through the Bowden tendon.

In the cam-spool system, a roller, which slides inside the spool, is coupled with a camshaft to vary the input elastic force. However, based on the working principle of the spool and the camshaft in Fig. 2, there is a challenge to rotate the spool for small angles. For instance, if a normal shaft

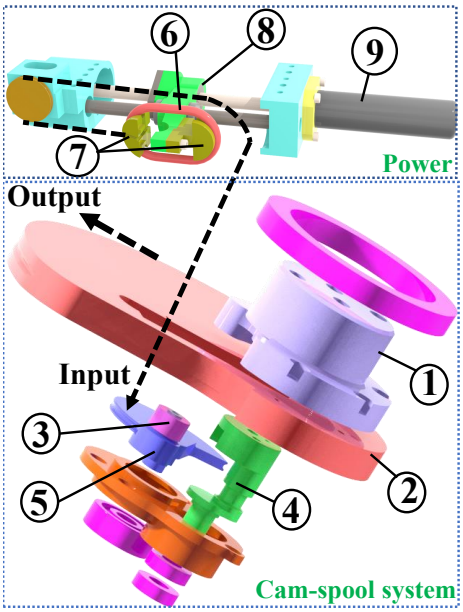

Fig. 6. Mechanical design of the assistive device. 1- Flange, 2- Spool, 3- Roller, 4- Eccentric shaft, 5- Camshaft, 6- Bungee, 7- Supports, 8- Plate, 9- Motor.

is coupled with the spool rotation axis (O_1) for the bedding purpose, the roller will not be able to approach to O_1 more than the diameter of this shaft. To address this issue, an eccentric shaft is developed not only for the bedding purpose of the spool but also for allowing the roller to approach O_1 at the small angles (see Fig. 6). With this new part, the operating range of the elbow and the spool is optimized to be between $9-116^\circ$, which is appropriate for manipulation tasks in industrial applications [19], [20]. In addition, a flange is designed and assembled from the upper side to align the spool and eccentric shaft on the same axis.

Finally, elbow-1 is fabricated and illustrated in Fig. 8 considering the human forearm dimensions and the location of the fixed attachments (see Fig. 2). Several holes are opened on this plastic elbow with 15° resolution to measure the torque variation in 7 test angles.

Regarding the open-end experiment, elbow-2 is manufactured, and an encoder is attached to this elbow (see Fig. 8). Another encoder, which is not illustrated in Fig.6 to reduce the complexity, is coupled with the flange part to compare if spool and elbow-2 achieve the same rotations.

To calculate the spool radius and the ball-screw stroke, two design parameters are assigned in Table.1 for the diameter of camshaft (R) and the working range of the elbow (θ_{max}). Using these parameters, the spool radius is computed as follows. Hence:

$$r_{spool} = \frac{l_f}{\theta_{max}} \tag{7}$$

Additionally, the tendon length wrapped around the camshaft is calculated to determine the necessary stroke in the ball-screw transmission of the power unit. As discussed before, the rotation angle of the camshaft is twice the spool rotation angle. Moreover, according to the geometrical derivation of the cam curve in Fig. 3, the radius of the cam is $|O_1O_2|$, which is equivalent to $R/2$. Therefore, the ball-screw stroke is calculated as follows:

$$S = (2\theta_{max})(R/2). \tag{8}$$

Considering an additional 20 mm tolerance for the elongation of the bungee, the ball-screw stroke is selected as 100 mm (see Table.1).

IV. Experiments and Results

Two experiments under fixed-end and open-end conditions were carried out using a 3D fabricated prototype (see Fig. 8) and presented in this section. In the first experiment, the elbow-1 was coupled rigidly with an F/T sensor (ATI-Mini45, SI 145-5), and they were both fixed to a table through apparatus. Center pins and screws were used to engage the elbow-1 and F/T sensor so that the applied assistive device force can be measured in different test angles. In the open-end experiment, the elbow-2 is free to rotate, and the aim is to measure the motion range of the assistive device.

A motor driver and a data acquisition card communicating through EtherCAT at 1kHz is used to control the assistive device. A PID regulator is used through MATLAB®/ Simulink Real-Time interface to drive the motor in power unit. The resultant linear position error on the ball-screw mechanism was detected between ± 0.15mm. Additionally, a 0.5 ± 0.1 Nm bias torque is maintained with the help of the assistive device in the fixed-end experiment to avoid relaxation on the cable and compensate for any backlash in the assembly.

TABLE I

Design parameters of the assistive device.

R (mm)	θ_{max}	r_{spool} (mm)	S (mm)
40	116°	88	100

A. Fixed-end

The force profile of the bungee is evaluated by tensioning the bungee between $0-10$ mm (0.5 mm position increment) in each predetermined elbow test angle ($15^\circ - 105^\circ$) and measuring the resultant torque around O_3 at elbow-1. These data are substituted into (2) as τ, and the estimated force profiles (F_d) are illustrated in Fig. 7. Furthermore, the average values of those estimated forces are calculated for each pretension value, and the resulting shape is demonstrated as "average" in the same figure. Finally, the same bungee is elongated (similar pretensions as elbow-1) using another tension machine. The measured force profile are reported as "desired" in the same figure.

According to the results in Fig. 7, the force profiles slowly rise in the beginning, then the trend sharply increases until 4% elongation, while for larger elongations the slope of the increment reduces. It is obvious that the differences in the force shapes among the test angles are insignificant, which indicates that the assembly of the components, cable connections and the force estimation based on (2) are achieved with minimal error. There is also an almost constant shift between desired and average force curves in most of the entire pretension points. This originates from the uncertainties of the plastic parts, such as stretching, manufacturing errors, as well as the friction in the cable.

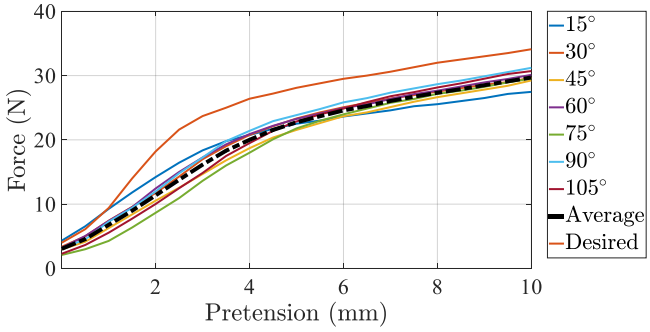

Fig. 7. Stiffness profile of an endless ring type of bungee (thickness ⌀5 mm and initial length 55 mm).

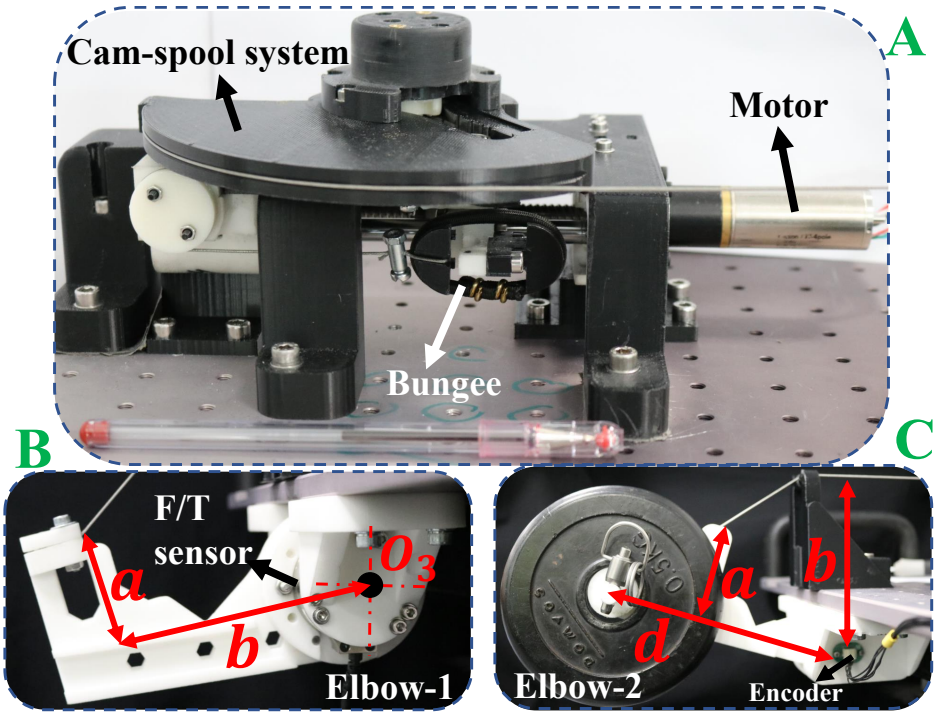

Fig. 8. The illustration of the 3D printed assistive device. A) Cam-spool system and power unit. B) Fixed-end experiment C) Open-end experiment.

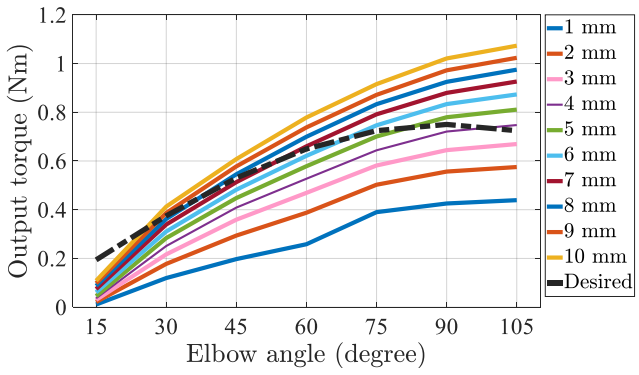

Fig. 9. Measured torque results of the fixed-end experiment, and the desired torque curve to balance 5N load in the forearm.

Next, the actuation system (i.e., power and cam-spool units) is tested to demonstrate the strength of the cam-spool mechanism. To implement that, first, the desired torque profile, which is expected to be delivered by the assistive device, is calculated by substituting 5N for W_l in (1). Then, the elbow-1 is configured and fixed mechanically in all the test points ($15^\circ - 105^\circ$) one by one, and the spool is rotated through the motor to the same position as that of the elbow-1. Subsequently, the bungee is tensioned, starting from 1 to 10 mm (1mm position increment) with the help of the motor in each test angle. Every pretension is repeated three times (standard deviation $\approx 0.1 - 0.0006$). Finally, the average values of those data are extracted from the bias torque, and reported in Table.2.

The graphical representation of the Table.2 is presented in Fig.9. There is a nonlinear increment as the elbow angle increases, which is an expected result based on the trend of h. However, there are fluctuations for 1 mm elongation curve. The reason is that since the transmitted force for that pretension is lower than others, the small relaxations on the cable, backlash between the assembled components, and frictions could not be compensated precisely.

Furthermore, according to the trend of h (see Fig. 5), it is expected to observe a slight reduction on the torque results between 90° to 105° (see Fig. 9). The reason why this behavior could not be detected is that the h difference between those two test angles is very low, and 7 test points are not adequate to validate the output torque of the assistive

TABLE II

Torque results of the assistive device. X and torque values are reported as mm and Nm unit, respectively.

θ_{spool}	15°	27°	40.9°	56.3°	73.2°	92.03°	109°
θ_{elbow}	15°	30°	45°	60°	75°	90°	105°
X=1.00	0.01	0.12	0.20	0.26	0.39	0.43	0.44
X=2.00	0.02	0.18	0.29	0.39	0.50	0.56	0.58
X=3.00	0.03	0.22	0.36	0.47	0.58	0.64	0.67
X=4.00	0.04	0.25	0.41	0.53	0.64	0.72	0.75⋆
X=5.00	0.05	0.28	0.45	0.58	0.70	0.78⋆	0.81
X=6.00	0.06	0.31	0.48	0.62	0.75⋆	0.83	0.87
X=7.00	0.07	0.34	0.51	0.66⋆	0.79	0.88	0.93
X=8.00	0.09	0.36	0.55⋆	0.70	0.83	0.92	0.97
X=9.00	0.10	0.39⋆	0.58	0.74	0.87	0.97	1.02
X=10.00	0.11⋆	0.41	0.61	0.78	0.92	1.02	1.07
Desired	0.19	0.37	0.53	0.64	0.72	0.75	0.72
Calibrated	0.16	0.45	0.59	0.73	0.77	0.79	0.73

⋆ Selected pretension values

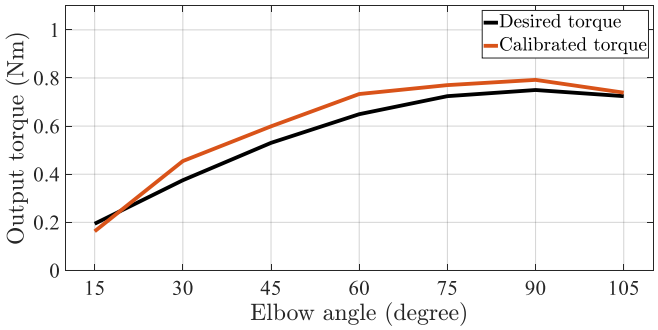

Fig. 10. The illustration of the selected pretension results to calibrate the assistive device to balance 5N load in a human hand.

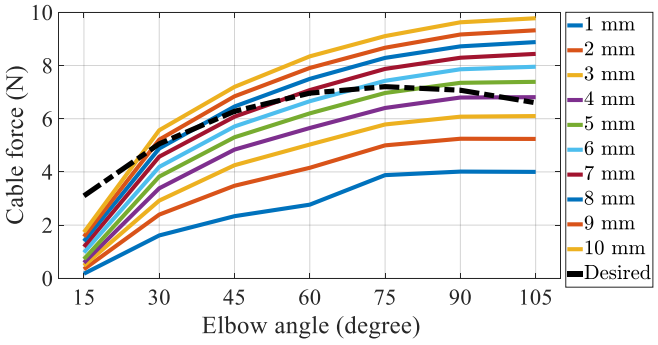

Fig. 11. Estimated cable force (F_d) of the fixed-end experiment, and the desired cable force to balance 5N load in the forearm.

device completely. Particularly, in Fig. 9, the increment ratio of the torque trends between $1-4$ mm elongation is significantly higher than that of the other pretensions. The aforementioned increment ratio is directly related to the stiffness curve of the bungee, which follows a sharp increase until 4 mm elongation, and then the slope of the force response reduces (see Fig. 7).

In the final step, the closest torque values to the desired ones are selected from Table.2, and the corresponding pretension values (X) are defined as "selected pretensions" for the calibration of desired torque profile. Those selected pretensions are applied to Elbow-1 in all the test angles. The results are written as "calibrated" in the same table, and the trend of them is presented in Fig.10. Noteworthy, since the elbow-1 is disassembled and assembled for the calibration, the small position shifts on the spool and the bias adjustments on the tendon lead to minor torque changes between selected pretensions and calibrated results.

Besides, it is observed from Table.2 that there is an angular position shift ($\approx \pm 4^\circ$) between the spool and the elbow, originating from the difficulty of precise position initialization of the elbow-1 and spool. Moreover, as discussed before, when the elbow angle is increased, h is supposed to rise as well, resulting to lower elastic force according to (5). This behavior is clearly observed in the Table.2 because the selected pretension values are significantly higher for 15° than for 105°.

Finally, in Fig. 11 shows F_d, which is calculated by substituting the measured torque values into (2) as τ.

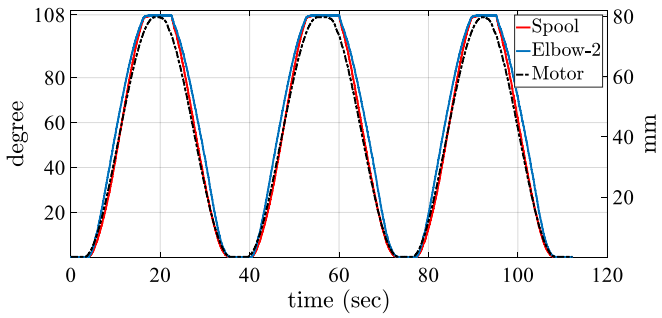

Fig. 12. The results of the open-end experiment. The right and left vertical axes illustrate the angular and linear position changes, respectively.

B. Open-end

In this test, a 0.5 kg load is mounted on the elbow-2, and the motor is driven to achieve the selected ball-screw stroke (see Table.1) for the flexion and extension movement. It can be seen in Fig. 12 that the position difference between the spool and the elbow is very low (RMS = 6.14°), which validates the proposed design concept. In addition, the measured angular position data verify the targeted kinematic working range of the elbow, which varies between $9-116^\circ$ ($\approx 108^\circ$).

V. Conclusions & Future Study

In this study, we presented the design of a novel actuation mechanism for an elbow assistive device. The power unit included a bungee as the elastic element to provide an intrinsically soft interaction between the actuation system and the elbow prototypes and to form a mechanical filter against dynamic uncertainties. Moreover, a new cam-spool mechanism was designed to optimize the force transmission effect between the elastic element and the assistive device's output.

Two tests were conducted on a 3D fabricated prototype to evaluate the motion and torque response of the assistive device. Results demonstrated that, although the bungee material exhibited an S-shape force response (see Fig. 7) causing a force fluctuations, the cam-spool system effectively adapted this shape to match the human torque profile with 90% success. In addition, as the elbow angle increased, the desired bungee pretension significantly reduced, which demonstrated the energy conversion during the flexion movement. These preliminary results gave solid evidence on the validity and utility of the proposed design concept. Future works will focus on the development of the final prototype, and its validation on multiple human subjects.

REFERENCES

[1] Y. Lee, J. Lee, B. Choi, M. Lee, S. Roh, K. Kim, K. Seo, Y. Kim, and Y. Shim, "Flexible gait enhancing mechatronics system for lower limb assistance (gems l-type)," *IEEE/ASME Transactions on Mechatronics*, vol. 24, no. 4, pp. 1520–1531, 2019.

[2] K. Schmidt, J. E. Duarte, M. Grimmer, A. Sancho-Puchades, H. Wei, C. S. Easthope, and R. Riener, "The myosuit: Bi-articular anti-gravity exosuit that reduces hip extensor activity in sitting transfers," *Frontiers in neurorobotics*, vol. 11, p. 57, 2017.

[3] T. Zhang and H. Huang, "A lower-back robotic exoskeleton: Industrial handling augmentation used to provide spinal support," *IEEE Robotics & Automation Magazine*, vol. 25, no. 2, pp. 95–106, 2018.

[4] N. C. Karavas, N. G. Tsagarakis, and D. G. Caldwell, "Design, modeling and control of a series elastic actuator for an assistive knee exoskeleton," in *2012 4th IEEE RAS EMBS International Conference on Biomedical Robotics and Biomechatronics (BioRob)*, 2012, pp. 1813–1819.

[5] B. Choi, Y. Lee, Y.-J. Kim, J. Lee, M. Lee, S.-g. Roh, Y. J. Park, K. Kim, and Y. Shim, "Development of adjustable knee joint for walking assistance devices," in *2017 IEEE/RSJ International Conference on Intelligent Robots and Systems (IROS)*. IEEE, 2017, pp. 1790–1797.

[6] N. G. Tsagarakis and D. G. Caldwell, "Development and control of a 'soft-actuated'exoskeleton for use in physiotherapy and training," *Autonomous Robots*, vol. 15, no. 1, pp. 21–33, 2003.

[7] K.-M. Lee and J. Guo, "Kinematic and dynamic analysis of an anatomically based knee joint," *Journal of biomechanics*, vol. 43, no. 7, pp. 1231–1236, 2010.

[8] B. Celebi, M. Yalcin, and V. Patoglu, "Assiston-knee: A self-aligning knee exoskeleton," in *2013 IEEE/RSJ International Conference on Intelligent Robots and Systems*, 2013, pp. 996–1002.

[9] M. A. Ergin and V. Patoglu, "A self-adjusting knee exoskeleton for robot-assisted treatment of knee injuries," in *2011 IEEE/RSJ International Conference on Intelligent Robots and Systems*, 2011, pp. 4917–4922.

[10] N. Vitiello, T. Lenzi, S. Roccella, S. M. M. De Rossi, E. Cattin, F. Giovacchini, F. Vecchi, and M. C. Carrozza, "Neuroexos: A powered elbow exoskeleton for physical rehabilitation," *IEEE Transactions on Robotics*, vol. 29, no. 1, pp. 220–235, 2013.

[11] T. Chen, R. Casas, and P. S. Lum, "An elbow exoskeleton for upper limb rehabilitation with series elastic actuator and cable-driven differential," *IEEE Transactions on Robotics*, vol. 35, no. 6, pp. 1464–1474, 2019.

[12] D. Chiaradia, M. Xiloyannis, C. W. Antuvan, A. Frisoli, and L. Masia, "Design and embedded control of a soft elbow exosuit," in *2018 IEEE International Conference on Soft Robotics (RoboSoft)*. IEEE, 2018, pp. 565–571.

[13] M. Xiloyannis, L. Cappello, K. D. Binh, C. W. Antuvan, and L. Masia, "Preliminary design and control of a soft exosuit for assisting elbow movements and hand grasping in activities of daily living," *Journal of rehabilitation and assistive technologies engineering*, vol. 4, p. 2055668316680315, 2017.

[14] M. Canesi, M. Xiloyannis, A. Ajoudani, A. Bicchi, and L. Masia, "Modular one-to-many clutchable actuator for a soft elbow exosuit," in *2017 International Conference on Rehabilitation Robotics (ICORR)*, 2017, pp. 1679–1685.

[15] B. W. K. Ang and C. H. Yeow, "Design and modeling of a high force soft actuator for assisted elbow flexion," *IEEE Robotics and Automation Letters*, vol. 5, no. 2, pp. 3731–3736, 2020.

[16] C. M. Thalman, Q. P. Lam, P. H. Nguyen, S. Sridar, and P. Polygerinos, "A novel soft elbow exosuit to supplement bicep lifting capacity," in *2018 IEEE/RSJ International Conference on Intelligent Robots and Systems (IROS)*, 2018, pp. 6965–6971.

[17] N. G. Tsagarakis, S. Morfey, H. Dallali, G. A. Medrano-Cerda, and D. G. Caldwell, "An asymmetric compliant antagonistic joint design for high performance mobility," in *2013 IEEE/RSJ International Conference on Intelligent Robots and Systems*. IEEE, 2013, pp. 5512–5517.

[18] W. T. Dempster and G. R. Gaughran, "Properties of body segments based on size and weight," *American journal of anatomy*, vol. 120, no. 1, pp. 33–54, 1967.

[19] D. Menychtas, A. Glushkova, and S. Manitsaris, "Analyzing the kinematic and kinetic contributions of the human upper body's joints for ergonomics assessment," *Journal of Ambient Intelligence and Humanized Computing*, vol. 11, no. 12, pp. 6093–6105, 2020.

[20] T.-H. Lee, "The effects of load magnitude and lifting speed on the kinematic data of load and human posture," *International Journal of Occupational Safety and Ergonomics*, vol. 21, no. 1, pp. 55–61, 2015.

[21] Z. Ren, W. Roozing, and N. G. Tsagarakis, "The eleg: A novel efficient leg prototype powered by adjustable parallel compliant actuation principles," in *2018 IEEE-RAS 18th International Conference on Humanoid Robots (Humanoids)*. IEEE, 2018, pp. 1–9.